Ab Initio Simulation of Molecular Beam Experiments for the F + H_2 → HF + H Reaction

F. J. Aoiz,* L. Bañares, and B. Martínez-Haya

Departamento de Química Física, Facultad de Química, Universidad Complutense, 28040 Madrid, Spain

J. F. Castillo[†] and D. E. Manolopoulos[†]

Department of Chemistry, University of Nottingham, Nottingham NG7 2RD, U.K.

K. Stark[‡] and H.-J. Werner

Institut für Theoretische Chemie, Universität Stuttgart, Pfaffenwaldring 55, D-70569 Stuttgart, Germany

Received: February 25, 1997; In Final Form: April 29, 1997[⊗]

The celebrated 1985 molecular beam measurements for the F + H_2 reaction of Lee and co-workers, consisting of time-of-flight (TOF) spectra and angular distributions (AD) at several collision energies, have been directly simulated using fully resolved differential cross-sections (DCS) obtained in accurate quantum mechanical (QM) and quasi-classical trajectory (QCT) calculations on the most recent *ab initio* potential energy surface (PES) by Stark and Werner. The simulations performed using the QM calculations show an unprecedentedly good agreement with the experimental results for all final vibrational states of the HF product. In particular, the height of the peak in the experimental laboratory angular distribution corresponding to HF(v'=3) forward scattering is quite well reproduced by the simulation using the QM theoretical data at all three experimental collision energies for both para and normal hydrogen. The most important discrepancies between theory and experiment are found in the HF(v'=3) sideways and backward scattering. The simulations carried out with the QCT data, although accounting correctly for the backward scattering, fail to account for most of the v' = 3 forward scattering. The analysis performed in this work indicates that an unbiased comparison between theoretical and experimental results in the laboratory frame (as opposed to the center-of-mass frame) is required to assess the quality of a theoretical calculation on a given *ab initio* PES.

I. Introduction

The F + H_2 → HF + H reaction has been a prototype and continuous reference in the field of reaction dynamics for decades and has played a key role in both theoretical and experimental studies of reactive scattering.[1]

A major breakthrough in the study of this reaction was achieved in the pioneering high-resolution molecular beam experiments reported by Lee and co-workers in 1985.[2,3] A series of systematic measurements at different collision energies allowed the authors to extract a very comprehensive picture of the dynamical behavior of the reaction. The resolution achieved in these experiments was unprecedented for the study of any reaction at the time, and remained so for several years. The results yielded fully vibrationally state resolved differential cross-sections at several collision energies for the F + H_2 reaction and its isotopic variants, which were elegantly presented as angle−velocity contour plots obtained following the suitable transformation from the laboratory (LAB) to the center-of-the-mass (CM) frame.

One of the most interesting dynamical features disclosed by these measurements was the appearance of forward scattering peaks in the CM differential cross-sections (DCS) for the HF(v'=3) product molecules formed in F + H_2 reactive encounters in the collision energy range between 0.7 and 3.4 kcal mol^{-1}. A smaller forward peak was also observed for the scattering of DF(v'=4) from F + D_2 at 3.32 kcal mol^{-1} collision energy.[3] For the rest of the vibrational states of HF and DF, the scattering was predominantly in the backward direction. At the time of the measurements no theoretical calculation, either classical[4−6] or quantum mechanical[4,7−11] on any of the existing surfaces and, most notably, on the widely used and strongly collinear M5 potential energy surface (PES),[12] could reproduce the state selective forward peaks observed in the experiments. Partly because of this, and also because of their apparent quantum state-specificity, these newly discovered features were regarded as the most promising evidence of a quantum mechanical (QM) resonance in the reactive scattering.[2,3] The discrepancies between experiment and theory were attributed to failures of the PES.

Since then, there have been continuous theoretical efforts to reproduce these experimental findings. The construction of new empirical[13] and semiempirical PES[14−17] allowed the qualitative reproduction of the DCS forward peaks in both quantum mechanical[17−19] and classical[13,20−23] dynamics calculations. After these works, it became generally accepted that the relevant PES for this reaction has a bent transition state and a comparatively flat angular barrier to reaction. Moreover, the fact that the DCS forward peaks also appeared in the quasi-classical trajectory (QCT) results cast serious doubts on their interpretation as a manifestation of QM scattering resonances. Nevertheless, the mentioned dynamical calculations on the new surfaces led to disagreements with other well-established experimental results, such as product state distributions,[2,3,24,25] reaction rate constants[26−28] and photoelectron spectra.[29−32]

Recently, a new and totally *ab initio* PES for this reaction has been constructed by Stark and Werner (hereafter SW).[33,34]

* Author to whom correspondence should be addressed.

[†] Present address: Physical and Theoretical Chemistry Laboratory, South Parks Rd., Oxford University, Oxford OX1 3QZ, U.K.

[‡] Present address: Fakultät für Physik, Universität Bielefeld, 33501 Bielefeld, Germany.

[⊗] Abstract published in *Advance ACS Abstracts,* July 1, 1997.

S1089-5639(97)00695-6 CCC: $14.00

Accurate QM calculations performed using this surface could account for the electron photodetachment spectra of the FH_2^- ion obtained by Neumark and co-workers,[35] which sample the transition state region of the potential energy surface. The asymptotic properties of reactive scattering on this PES have also been investigated. QCT calculations for the F + H_2 system and its isotopic variants on the SW PES[33,36−38] have revealed substantial accordance with the experimentally deduced CM differential cross-sections and with the product state distributions reported by Lee and co-workers for the F + H_2 reaction and its isotopic variants,[2,3] as well as with the recent higher resolution data of Faubel *et al*. on the F + D_2 reaction.[39−42] In particular, the tendency from backwards to sideways peaking of HF(v'=2) scattering with increasing collision energy and the forward peaks in the DCS of HF(v'=3), which had been succesively attributed to QM resonances, are obtained in these classical calculations. The results of the mentioned QCT calculations on the SW PES seemed to yield a global agreement with the experimental data in the CM frame.

However, a noteworthy difference between the experimentally deduced DCS for F + H_2 and those from QCT calculations on the SW surface persisted. The theoretical forward peaks were significantly smaller than in the experimental case.[33] Subsequent accurate QM calculations performed by Castillo *et al.*[43] on the SW PES showed that the forward peaks were very much increased in quantum calculations. This was also indicated by an earlier comparison of QCT and exact QM differential cross-sections for the F + H_2(j=0,1) reaction on the semiempirical 6SEC PES,[17,22] where the classical forward peaks were again much enhanced in the quantal calculation. Furthermore, the forward scattering of HF(v'=3) in the CM frame seemed to be substantially more pronounced than in the experiment although confined to a narrower range of CM scattering angles.[43] In addition, the calculations predicted a nonnegligible forward scattering for $v' = 2$. The analysis of the forward scattering in both QCT and QM calculations indicates that it is associated with the largest accesible orbital angular momentum that can yield reaction. In the QM case, Manolopoulos and co-workers[43] showed that tunneling for high angular momenta, which are not accessible classically, through the combined centrifugal and potential energy barrier is the sole reason for the enhancement of the $v' = 3$ forward peak found in the QM calculation. In addition, the analysis of time delays indicates that the peak found in the QM cumulative reaction probability for $J = 0$, responsible at higher angular momenta of the QM $v' = 3$ forward scattering, does not correspond to a time delay maximum. Therefore, all theoretical evidences seem to rule out the original interpretation of the $v' = 3$ forward scattering as a manifestation of a reactive scattering resonance.

Except for in a very few recent cases,[44,45] the experimental data obtained in the laboratory frame are not well enough resolved to provide a unique and unambiguous set of results in the CM frame. In previous works,[37,38] where the molecular beam experiments on the F + HD and F + D_2 isotopic variants of the reaction were compared with the results of QCT calculations on the SW PES, the importance of carrying out the simulation of direct experimental observables in the LAB frame to assess the reliability of the theoretical calculation was clearly demonstrated. To date, no such attempt has been made for the simulation of the F + H_2 raw molecular beam experimental data of Neumark *et al.*,[2] *i.e.* HF product angular distributions and time-of-flight spectra in the LAB frame. The availability of high-quality QM[43] and QCT[33] theoretical results on a high-quality *ab initio* PES[34] provides a unique opportunity to carry out such a comparison. The relevant results in the CM frame have been already published and discussed elsewhere,[33,43] and what remains now is to check the capability of the theoretical calculations to reproduce the experimental observables. It will be shown that this comparison clearly leads to a better assessment of the theoretical results (*ab initio* PES and dynamical calculations) than a comparison in the CM frame.

The paper is organized as follows: section 2 gives a description of the methodology used for the simulation of the molecular beam experimental results using the QM and QCT DCSs calculated on the SW PES. Section 3 contains the results of these *ab initio* simulations and the comparison with the experimental angular distributions and time-of-flight spectra. Some conclusions are given in section 4.

II. Method

The methodology presented here is appropriate for the simulation of direct observables of a crossed molecular beam scattering experiment in the laboratory system from theoretically calculated rovibrational (v',j') differential cross-sections in the CM frame. The experiments to be considered here are those of Lee and co-workers on the F + H_2 reaction[2] performed with continuous molecular beams and mass spectrometric product detection, either as a function of the flight time (time-of-flight spectra, hereafter TOF) or integrated at a given LAB scattering angle over all arrival times (laboratory angular distribution, hereafter LAB AD). The simulations have been performed using the QM v',j' resolved DCSs calculated by Castillo *et al.* on the SW PES[43] and the QCT v',j' DCSs calculated by Aoiz *et al*. on the same PES.[33]

The simulation procedure is similar to that applied before[36−38] for similar experiments carried out by Neumark *et al*.[3] on the F + D_2 and F + HD reactions and by Faubel *et al.*[39,42] on the F + D_2 reaction, employing v',j' resolved DCS obtained in QCT calculations on several PESs.[33,37,38]

A. Simulation of Time-of-Flight Spectra and Laboratory Angular Distributions. The simulation of the TOF spectra of the scattered HF molecules is carried out by transforming the theoretical CM v',j' DCSs into the LAB system[46] and performing the convolution with the experimental distributions of beam velocities and divergences and detector aperture. In short, the signal detected at a given time t and LAB scattering angle Θ_{LAB} can be expressed as[37,42]

$$I(t;\Theta_{LAB}) = \sum_j P(j) \int d^3\mathbf{r} \int\int dv_1\, dv_2 \int d\Omega\, D(\Omega,\Theta_{LAB}) \times f(v_1)\, f(v_2)\, n_1(\mathbf{r})\, n_2(\mathbf{r}) v_r \sum_p \sum_{q=1,2} \left(\frac{d^2\sigma}{d\omega}\right)_p \frac{v_{pq}^{\,2}}{w_p^{\,2}|\cos \xi_{pq}|} \frac{t_{pq}}{L} \times H[t_{pq} - (t_0 - \delta)]\, H[(t_0 + \delta) - t_{pq}] \quad (1)$$

The different integrals are performed by a Monte Carlo sampling of the reagent beam velocities v_1 and v_2 with distributions $f(v_1)$ and $f(v_2)$ and spatial beam densities $n_1(\mathbf{r})$ and $n_2(\mathbf{r})$, where the position vector $\mathbf{r}$ refers to a point in the scattering volume defined by the beam divergences and the geometry of the experiment.[2] In this equation, v_r is the relative velocity, v_{pq} and w_p are the LAB and CM velocities of the HF product, respectively, and ξ_{pq} is the angle between v_{pq} and w_p. The summation over p extends to all the final rovibrational v',j' states energetically accessible. The summation over $q = 1, 2$ takes into account the fact that, for a given quantum state of the products, there might be, at a given Θ_{LAB}, both fast and slow products in the LAB system (see the Newton diagram in Figure 1). The factor $1/v_{pq} = t_{pq}/L$ accounts for the fact that the detected signal is proportional to the number density of the HF product molecules,[46] where t_{pq} is the time of flight of the products formed in the p state before ionization and L is the

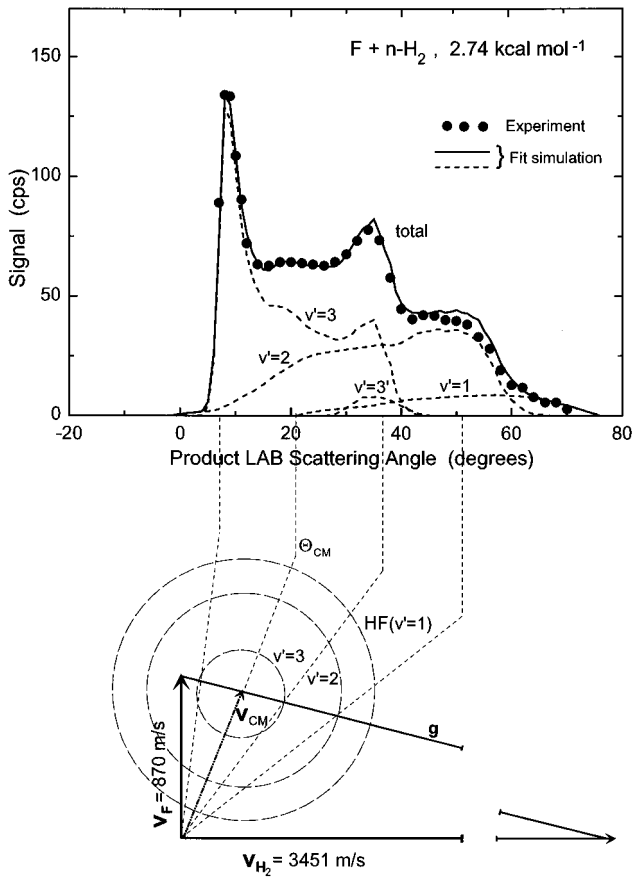

Figure 1. (Top) Experimental HF product density laboratory angular distribution (LAB AD) at 2.74 kcal mol^{-1} collision energy. The solid points are the experimental data. The solid line is the simulation carried out with the experimentally extracted center-of-mass parameters[2] using the methodology of the present work. The dashed lines are the v' resolved contributions to the LAB AD, including the $v' = 3'$ state (see text). Signal is in counts-per-second (cps). (Bottom) Nominal kinematic (Newton) diagram at this collision energy.

flight length. The Heavyside step functions, $H(x)$ (equal to 1 if $x > 0$ and equal to 0 if $x < 0$), are used to indicate that only those times t_{pq} within the interval $(t_0 - \delta, t_0 + \delta)$, where $2\delta =$ 8 μs/channel (the counting time resolution),[2] are included in a given channel. The final time t is the sum of t_0, the neutral HF flight time from the chopper (located at the entrance of the flight tube of the detector) to the ionization region and t_i, the HF^+ ion time of flight inside the mass spectrometer. Finally, $D(\Omega,\Theta_{LAB})$ accounts for the cone of acceptance of the detector (aperture of 1.25° full width at half-maximum (fwhm)). The experimental parameters for the simulation have been directly taken from ref 2, and a flight length L of 33 cm was used.[47]

The LAB ADs are simulated in a similar way as the TOF spectra. The total reactive signal detected at a given scattering angle, $S(\Theta_{LAB})$, is obtained by integrating eq 1 over time[37,42,46] as follows:

$$S(\Theta_{LAB}) = \sum_j P(j) \int d^3\mathbf{r}\, n_1(\mathbf{r})\, n_2(\mathbf{r}) \int d\Omega\, D(\Omega,\Theta_{LAB}) \int\int dv_1\, dv_2 \times f(v_1)\, f(v_2) v_r \sum_p \sum_{q=1,2} \left(\frac{d^2\sigma}{d\omega}\right)_p \frac{v_{pq}}{{w_p}^2 \cos \xi_{pq}} \quad (2)$$

The results of the different simulations of both the LAB ADs and TOF spectra have been obtained by appropriately weighting on the initial rotational quantum number j of the H_2 reagent, as indicated in eqs 1 and 2 via the summation over j. The corresponding weights, $P(j=0,1,2)$, are listed in Table 1 and have been obtained by linear interpolation of previously measured rotational populations of H_2 molecules in supersonic beams[48] under similar expansion conditions as those used in the crossed beam experiments of Neumark *et al.*[2] Since no QM calculations have been carried out for initial rotational states $j \geq 3$, their estimated relative populations were included in ($j = 2$) in the simulations. This seems to be a good approximation given the similarity of the QCT DCSs obtained for $j = 2$ and $j = 3$ and the low contribution from $j = 3$.

TABLE 1: Estimated Rotational Temperatures, $T_{rot.}$, and Relative Rotational Populations, $P(j)$, of the H_2 Reagents in the Experiments of Neumark *et al.*

reactants	E_{CM} (kcal mol^{-1})	$T_{rot.}$ (K)	$P(j=0)$	$P(j=1)$	$P(j=2)$	$P(j\geq 3)$
F + *p*-H_2	1.84	170	0.80	0.00	0.20	0.00
F + *n*-H_2	1.84	170	0.20	0.74	0.05	0.01
F + *n*-H_2	2.74	260	0.15	0.69	0.10	0.06
F + *n*-H_2	3.42	325	0.12	0.64	0.12	0.12

The whole set of experimental data were taken by scanning the figures of refs 2 and 49. The measured LAB ADs were given in units of counts-per-second (cps), whereas the experimental TOF spectra were given in arbitrary units.[2,49] To obtain the latter in units of counts-per-second-per-channel (cps/ch), as shown in the figures of the present work, and to match the relative total reactive signal as a function of the LAB scattering angle, every experimental TOF spectrum at a given LAB scattering angle was integrated in time and the result was equated to the point of the published LAB AD at that angle.

Since absolute values for the reactive cross-sections were not reported in the scattering experiments of Neumark *et al.*,[2] a direct comparison between the theoretical predictions and the measurements requires an additional global factor in order to scale both the simulated TOF spectra and LAB ADs to the experimental ones. This scaling factor was determined in the present work by performing a least squares fit of the corresponding LAB AD in order to minimize the difference between the QM calculated and measured data. The resulting scaling factor, C, is given by $C = \sum_i (w_i S_i^{exp} S_i^{theor}) / \sum_i w_i (S_i^{theor})^2$, where $S_i^{exp}(\Theta^i_{LAB})$ and $S_i^{theor}(\Theta^i_{LAB})$ are the experimental and QM simulated reactive signals, respectively, at a given LAB scattering angle Θ^i_{LAB}, and w_i is the relative weight of each experimental point in the LAB AD which is given by the inverse of the statistical variance of the counting rate, $1/S_i^{exp}$, assuming a Poison distribution ($\sigma_i^2 = S_i^{exp}$). For each of the four scattering experiments here considered (F + *p*-H_2 at 1.84 kcal/mol and F + *n*-H_2 at 1.84, 2.74, and 3.42 kcal/mol collision energies) the factor C was obtained by scaling the simulated QM LAB AD to the experimental one. The same factor was also used in each case for the respective simulation with the QCT DCSs, since the QCT and QM calculations are directly comparable.

Other scaling criteria have also been tested, such as, for instance, equating the areas of the experimental and simulated LAB ADs in the range of angles scanned by the experiment. Since the integral of the LAB AD is not a cross-section (the LAB AD intensities are proportional to the HF number density rather than to the product flux), there is no reason why this scaling should be preferred to that based on the counting rates for each measured point. In any case, the scaling factors resulting from both procedures were found to agree to within 5−10%.

In order to test the reliability of the method, the LAB AD of the HF products and four representative TOF measurements from the experiment with F + *n*-H_2 at 2.74 kcal mol^{-1} collision energy were simulated by employing the experimental CM state

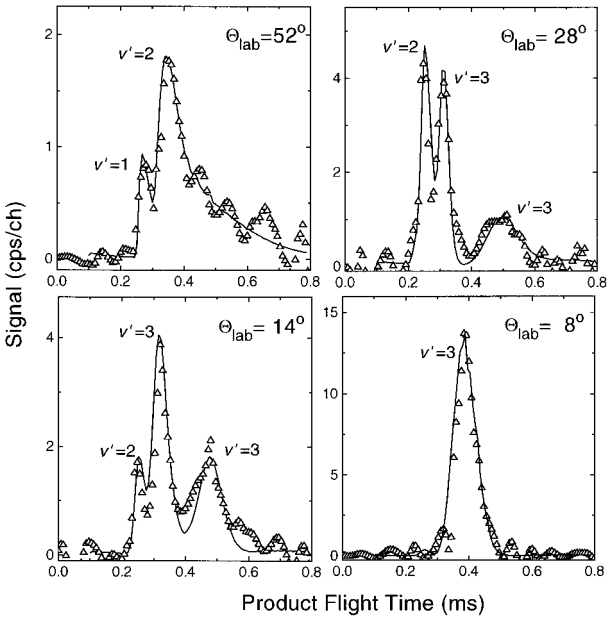

Figure 2. Experimental time-of-flight spectra at 2.74 kcal mol^{-1} collision energy at the indicated LAB scattering angles: triangles, experimental data; solid line, present simulation with the experimentally extracted center-of-mass parameters.[2] Signal is in counts-per-second-per-channel (cps/ch) (see text).

resolved differential cross-sections evaluated by Neumark *et al*. (Figure 16 of ref 2). As can be seen from Figure 1, the simulation of the LAB AD performed using our method reproduce perfectly the results in Figure 11 of ref 2 when the same CM data are used. Similarly, the four TOF simulations shown in Figure 2 resemble very closely those obtained by Neumark *et al*. (Figure 11 of ref 49). It must be mentioned here that the simulations in Figures 1 and 2 were performed following the approach of Neumark *et al*.,[2] wherein it is assumed that all the H_2 molecules are initially in the most probable rotational state $j = 1$ and, additionally, a small contribution is included from an extra "state" labeled $v' = 3'$. In order to get a good fit of their experimental results, Neumark *et al*. were forced to postulate this $v' = 3'$ state, corresponding to HF(v'=3) formed from reactants with about 1 kcal mol^{-1} of internal excitation (see the Newton diagram in Figure 1)[2] whose scattering would be confined in the backward region. As pointed out by the authors of ref 2, the possible sources for the extra energy could be contributions to the reaction from (a) the spin−orbit excited F($^2P_{1/2}$) nonadiabatic channel or (b) rotationally excited H_2. The possible contribution of the nonadiabatic channel to the reaction cannot be ruled out completely, and, in fact, some evidence for it has been found in the molecular beam experiments carried out in Göttingen on the F + D_2 reaction.[39,40] However, if present, and in analogy with the results obtained for the F + D_2 reaction, this contribution is expected to be very small in comparison with the ground state adiabatic channel and confined into a still narrower range of scattering angles.[39] The second hypothesis is the most likely, but in any case is already taken into account in our simulations by using the DCSs for initial $j = 2$ appropriately weighted (*ca*. 20% for *p*-H_2). Therefore, in the following simulations with the theoretical (QCT and QM) results, the hypothetical $v' = 3'$ state has been omitted.

B. Polar Maps. In the absence of a privileged quantization axis (such as an external field), the maximum information in the CM frame consists of a complete set of rovibrationally state resolved DCSs, as given by either of the calculations used in the present work (QCT or QM), from which the results in the LAB frame can be simulated. However, the experimental results

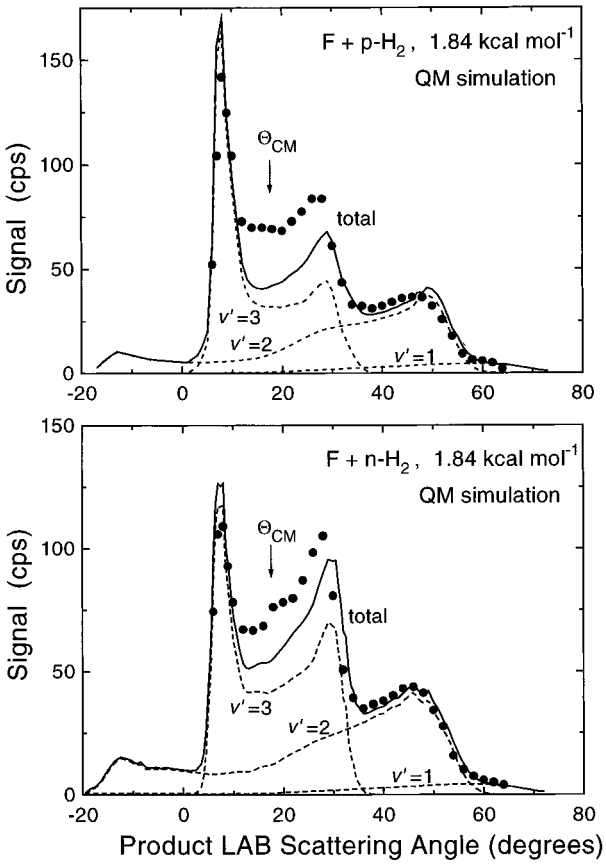

Figure 3. Comparison between the experimental (solid points) and the theoretical (solid line) LAB ADs using the quantum mechanical v',j' resolved differential cross-sections of ref 43 at 1.84 kcal mol^{-1}: (top) F + *p*-H_2; (bottom) F + *n*-H_2. The dashed lines are the simulated contributions of the different v' states to the total LAB AD. The position of the average centroid angle Θ_{CM} is indicated with an arrow.

did not allow the determination of individual v',j' CM differential cross-sections, and the CM results were cast, instead, in terms of angle−velocity contour polar maps (triple angle−velocity DCSs).

In order to construct polar maps from the theoretically calculated CM v',j' state resolved DCSs that are directly comparable with the ones reported in ref 2, some broadening needs to be included to account for the lack of rotational resolution in the experiment. To a good approximation, this broadening can be incorporated by assuming a Gaussian spread in the products CM recoil velocity. The CM angle−velocity DCS at a CM scattering angle θ is then

$$P(w,\theta) = \sum_j P(j) \sum_k \left(\frac{d^2\sigma}{d\omega}\right)_k N_k \exp\left[-\left(\frac{w - w_k}{\Delta w_k}\right)^2\right] \qquad (3)$$

where the first sum over j accounts for the averaging over initial H_2 rotational states and the sum over k extends to all the final v',j' HF states which are energetically accessible. The experimental resolution in w is thus modeled with a Gaussian distribution centered in every case at w_k, the recoil velocity associated with the internal state k. The N_k are the normalization constants of the Gaussian profiles. The fwhm, given by $2(\ln 2)^{1/2}\Delta w_k/w_k$, was 10−12% in all cases, corresponding to a HF CM energy resolution of 20−24%. This procedure was used in previous works to obtain the corresponding QCT polar maps.[33]

III. Results and Discussion

A. Laboratory Angular Distributions. Figures 3 and 4 show the comparison between the experimental LAB AD of

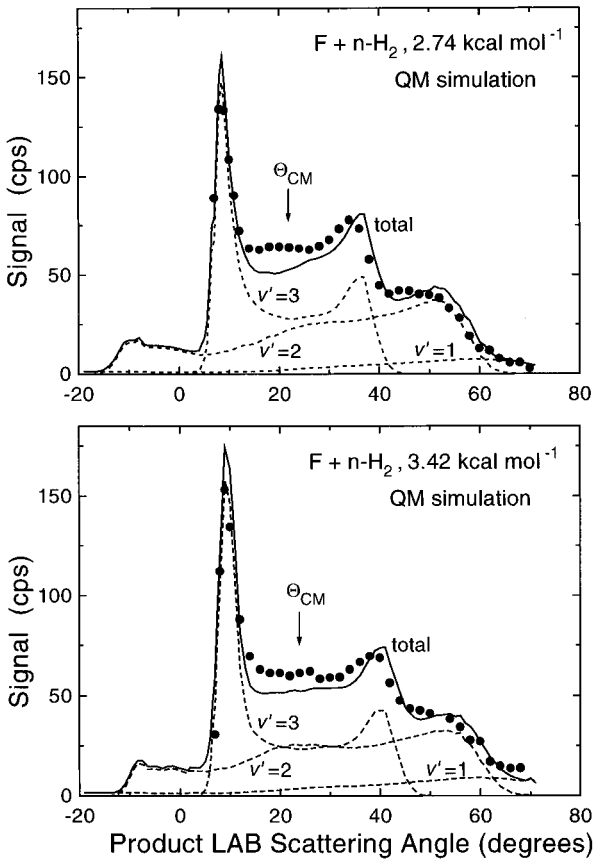

Figure 4. As in Figure 3, but for the F + *n*-H_2 reaction at 2.74 kcal mol^{-1} (top) and 3.42 kcal mol^{-1} (bottom) collision energies.

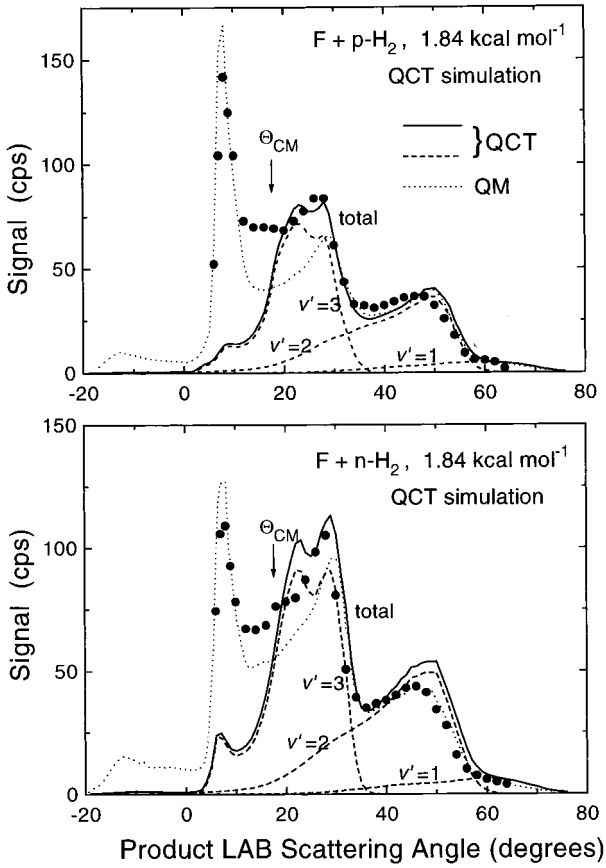

Figure 5. Comparison between the experimental (solid points) and theoretical (solid line) LAB ADs using the quasi-classical v',j' resolved differential cross-sections of ref 33 at 1.84 kcal mol^{-1}: (top) F + *p*-H_2; (bottom) F + *n*-H_2. The dashed lines are the simulated contributions of the different v' states to the total LAB AD. For reference purposes, the corresponding total QM LAB AD is depicted as a dotted line. The scaling factor is the same for the two theoretical simulations.

the HF products measured by Neumark *et al.*[2] and the simulations carried out using the QM scattering calculations of Manolopoulos and co-workers on the SW PES.[43] The simulated AD at each collision energy has been independently scaled to the experimental points by means of a least squares fit, as described in section II. Each theoretically simulated AD is resolved into the contributions from the different final HF vibrational states, which are shown as dashed lines in the figures. In addition, the theoretical simulations of the LAB ADs have been extended to negative LAB angles not reported in the experimental measurements where the forward scattering from $v' = 2$ appears. The centroid angle, Θ_{CM}, *i.e.* the LAB angle corresponding to the velocity of the center-of-mass of the three atoms, is indicated with an arrow in the upper part of each figure. This angle roughly divides the LAB scattering space into a low-angle hemisphere, associated with forward scattering in the CM frame, and a high-angle hemisphere where CM backward scattered HF products are detected (see the Newton diagram in Figure 1).

The structure of the experimental LAB ADs is qualitatively very similar in the four cases considered (F + *p*-H_2 at a collision energy of 1.84 kcal mol^{-1} and F + *n*-H_2 at 1.84, 2.74, and 3.42 kcal mol^{-1}). It should be noted that the signal in the LAB ADs is proportional to the HF number density rather than to the flux. Therefore, the contribution of the highest vibrational states (smaller LAB velocities) to the AD is enhanced with respect to that from the lower states, and this fact together with the kinematics of the experiment, which confines the $v' = 3$ scattering to a small angular range, results in a better detection of the HF(v'=3) scattering. Thus, the most pronounced feature in the ADs is the prominent peak at small LAB angles (Θ_{LAB} between 8 and 10°), which is associated mainly with CM forward scattered HF(v'=3) product molecules. In addition, all the LAB ADs show two more peaks at $\Theta_{LAB} \approx 30$ and 50°, which are associated with CM backward scattering from HF(v'=3) and HF(v'=2), respectively. The relative heights and locations of the peaks change substantially from experiment to experiment, due to both the different kinematics and the different reactive state-to-state differential cross-sections.

In general, the simulations performed using the QM DCSs calculated on the SW PES reproduce the main trends in the experimental LAB ADs. The agreement is remarkably good at the largest LAB scattering angles ($\Theta_{LAB} > 40°$). Similar agreement in the backward region is found in the CM frame between the experimental and QM DCSs for $v' = 1$ and $v' = 2$ (see ref 43). On the other hand, the main discrepancies between experimental and theoretical results are found in the angular region between 6 and 30° and are mostly attributable to scattering into HF(v'=3). In particular, the forward peak seems to be somewhat overestimated in the theoretical simulations, and, more importantly, the $v' = 3$ sideways and backward scattering predicted theoretically is smaller than in the experiment. As the collision energy increases, there seems to be a better agreement between theory and experiment.

Figure 3 shows the experimental and QM simulated LAB ADs for the F + *p*-H_2 and F + *n*-H_2 reactions at the collision energy 1.84 kcal mol^{-1}. For the F + *p*-H_2 reaction, the most populated H_2 rotational state is $j = 0$ (80%; see Table 1), whereas for F + *n*-H_2 it is $j = 1$ (74%). The experimental LAB AD is strongly sensitive to the different initial rotational population of the H_2 molecules. Clearly, for the F + *n*-H_2 reaction, the forward peak is lower and the $v' = 3$ and $v' = 2$ backward peaks are larger than for the F + *p*-H_2 reaction, and these features are well-reproduced by the theoretical simulation. Although in both cases the forward peak ($\Theta_{LAB} \approx 6-12°$) seems

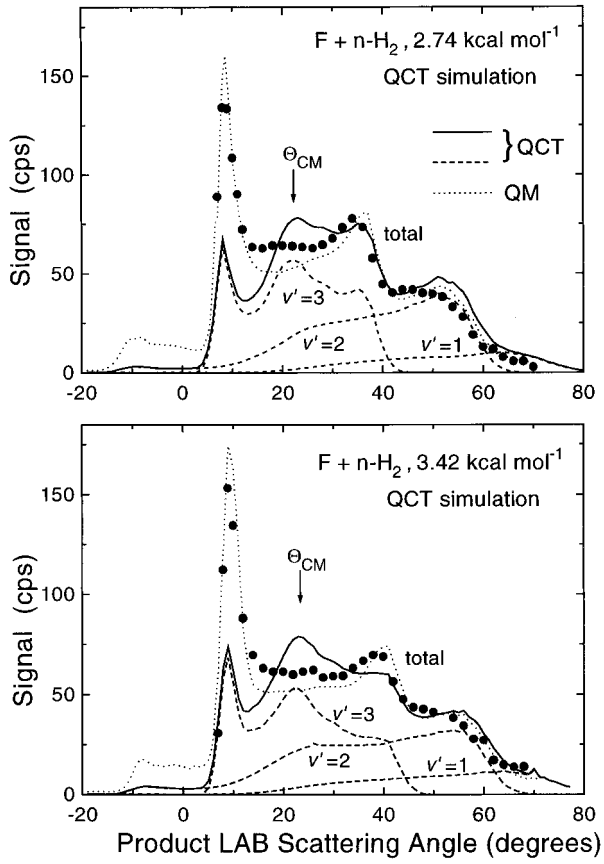

Figure 6. As in Figure 5, but for the F + n-H_2 reaction at 2.74 kcal mol^{-1} (top) and 3.42 kcal mol^{-1} (bottom) collision energies.

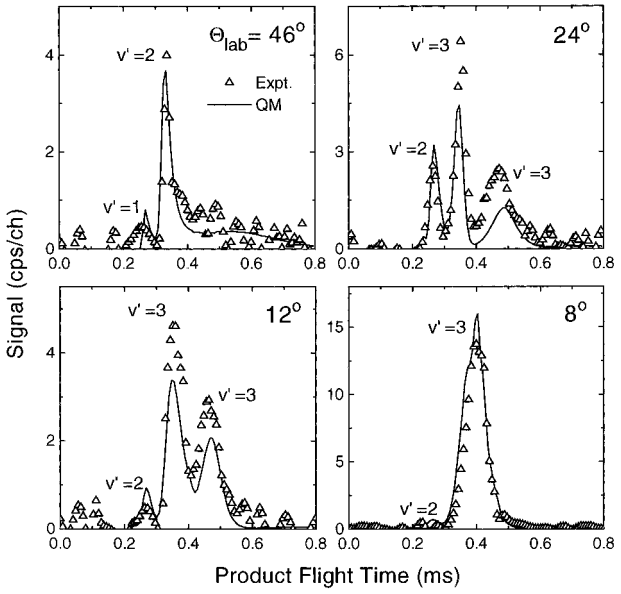

Figure 7. Time-of-flight spectra at several selected LAB angles for the F + p-H_2 reaction at 1.84 kcal mol^{-1}: triangles, experimental data; solid line, present simulation using the quantum mechanical v',j' resolved differential cross-sections of ref 43. In each TOF spectrum the peaks corresponding to each v' are indicated. The ordinate scale is in counts-per-second-per-channel (cps/ch), such that the integrated signal coincides with the the counting rate obtained in the LAB AD at each angle.

to be slightly overestimated, an inspection of the v' resolved LAB ADs indicates that the main discrepancies between the theoretical and experimental ADs can be traced to the HF(v'=3) CM sideways and backward scattering. This is somewhat surprising since a simple comparison of the theoretical and experimentally extracted $v' = 3$ CM DCSs (see Figure 1 of ref

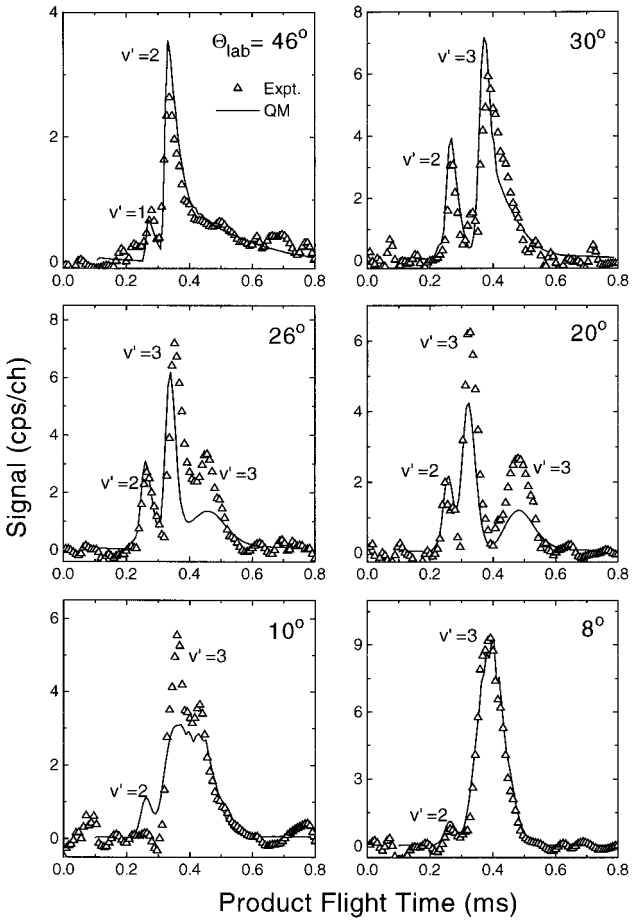

Figure 8. As in Figure 7, but for the F + n-H_2 reaction at 1.84 kcal mol^{-1} collision energy.

43) would lead to the conclusion that it is in the height of the forward peak where the main discrepancy appears. It should be noticed, however, that the theoretical CM forward peak is narrower (more confined in the forward region) than the experimental peak. Given the limited resolution of the experiment, a broader but smaller CM forward peak, more like the one evaluated from the measurements, would yield very similar results in the LAB system. On the other hand, a close inspection of the $v' = 3$ CM DCS reveals that the sideways scattering (θ_{CM} = 40−90°) is smaller in the QM calculation than in the experiment, and this is readily apparent when the simulation is performed in the LAB frame. These findings clearly illustrate the advantage of carrying out the simulation of direct experimental observables in the laboratory frame for an appropriate appraisal of the theoretical results.

The $v' = 3$ backward scattering, which corresponds to the peak at ≈30° in the LAB system, is also clearly underestimated in the QM simulation, especially for the F + p-H_2 reaction. When the comparison is carried out in the CM frame, this lack of backward scattering is not obvious (see Figure 1 of ref 43). It should be recalled, however, as mentioned in section II, that Neumark *et al*. included a ficticious $v' = 3'$ state, presumably related to the participation of H_2 (j>1), to fit their experimental data; the scattering from this state would appear in this region in the LAB system and would add to the contribution from v' = 3. At higher collision energies (see below) the $v' = 3$ backward scattering is very well accounted for by the theoretical calculations. In any case, the inclusion of $v' = 3'$ scattering in the experimental analysis does not remove the discrepancy found at smaller Θ_{LAB} angles, corresponding to $v' = 3$ sideways scattering, which seems to remain, although to a lesser extent, at higher energies. It is gratifying to see that the increase of v'

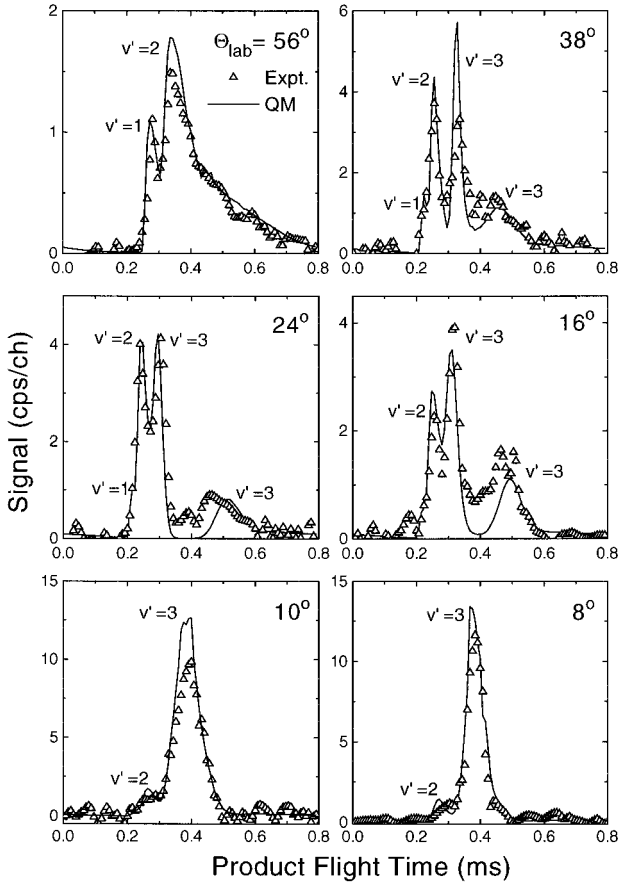

Figure 9. As in Figure 7, but for the F + *n*-H_2 reaction at 3.48 kcal mol^{-1} collision energy.

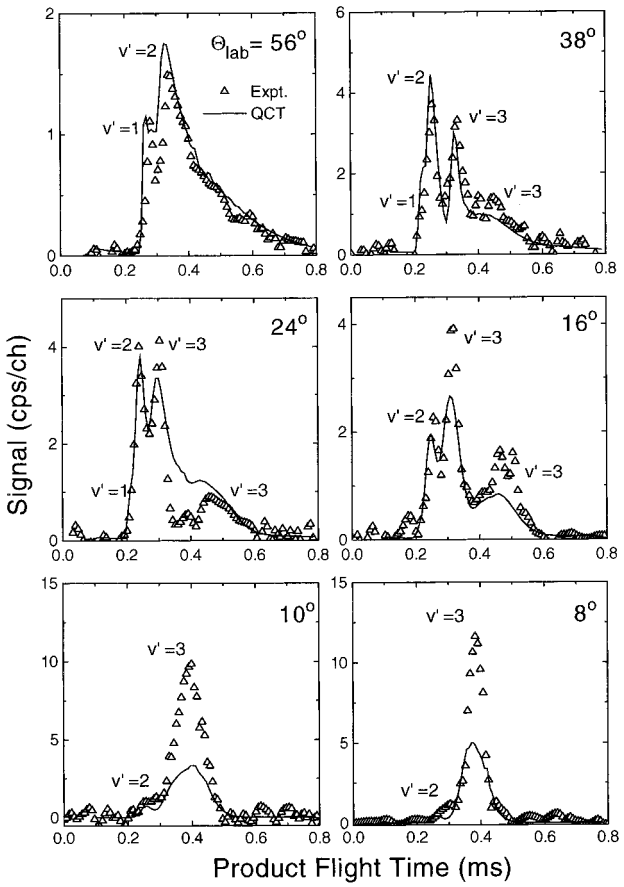

Figure 10. Time-of-flight spectra at several selected LAB angles for the F + *n*-H_2 reaction at 3.42 kcal mol^{-1}: triangles, experimental data; solid line, present simulation using the quasi-classical trajectory v',j' resolved differential cross-sections of ref 37.

= 3 backward scattering in going from *p*-H_2 to *n*-H_2 is theoretically well accounted for by the partipation of higher *j* states in the reaction; however, the present QM calculations cannot reproduce quantitatively the scattering in this region in spite of including an appropriate weighting in initial *j* quantum number.

It is interesting to notice that the QM simulations lead to a better overall agreement with the experimental AD for the F + *n*-H_2 reaction than for the F + *p*-H_2 reaction. This fact can be taken as an indication that the dynamics on the SW PES for the F + $H_2(j \geq 1)$ reaction performs better than for the reaction from ground state hydrogen.

The QM simulated LAB ADs for the F + *n*-H_2 reaction at the higher collision energies 2.74 and 3.42 kcal mol^{-1} are shown in Figure 4. Overall, the agreement between the results of the QM simulation and the experiment improves as the collision energy increases. The QM calculations account for the $v' = 3$ sideways and backward scattering at these energies significantly better than in the experiments at 1.84 kcal mol^{-1}. However, the forward peak is still somewhat overestimated in the LAB ADs. Although the height of this peak in the QM calculation is mainly determined by CM $v' = 3$ forward scattering, as in the experiment, it also contains a significant contribution from HF(v'=2) scattered at small CM angles ($\theta_{CM} = 20-50°$). This is in contrast with the analysis of the experimental data, which assigned a lower fraction of HF products in $v' = 2$ in this interval of LAB angles (see Figure 1, ref 2). It will be shown in the simulations of the TOF spectra (see below) that the $v' = 2$ scattering theoretically predicted in this range of LAB angles is, however, not incompatible with the experimental measurements.

The above discussion leads to the important question of the product state specificity of the CM forward scattering, which is dominated by HF(v'=3) scattered product molecules. The Newton diagram shown in Figure 1 indicates that the HF(v'=2) forward scattering would appear at negative LAB angles, on the other side of the F atom beam. In this angular region, although accessible to the rotatable detector, the experiment showed no evidence of a measurable signal. It was concluded that a negligible v'=2 forward scattering was produced at all measured collision energies and that all the forward scattering was specifically associated with $v' = 3$. Indeed this apparent quantum state specificity was one of the original reasons for the interpretation of the $v' = 3$ forward scattering as a QM resonance. However, all the QCT and accurate QM calculations carried out on PESs with bent transition states and flat angular barriers indicate the presence of a minor forward scattering contribution from $v' = 2$.[17−19,43] Specifically, the QM calculations on the SW PES[43] give rise to a nonnegligible contribution from $v' = 2$ to the total forward scattering, which is approximately independent of the collision energy. The question is whether the $v' = 2$ forward scattering predicted theoretically would have been detectable under the experimental conditions of Neumark *et al.*,[2] especially if one takes into account the fact that the kinematics is less favorable for the detection of $v' = 2$ forward scattering and that this scattering will be more dispersed in the LAB system than that of $v' = 3$ (see above). The simulations of the LAB AD shown in Figures 3 and 4 also contain the range of LAB angles where the forward $v' = 2$ scattering would appear, and indeed there is a shallow maximum at a LAB angle of *ca.* −12° at all collision energies. The most extreme case appears to be that of the F + *n*-H_2 reaction at 1.84 kcal mol^{-1}, where the ratio of the peak heights for forward $v' = 3$ and $v' = 2$ scattering is only about a factor 8. The hypothetical signal in the $v' = 2$ forward peak predicted by the

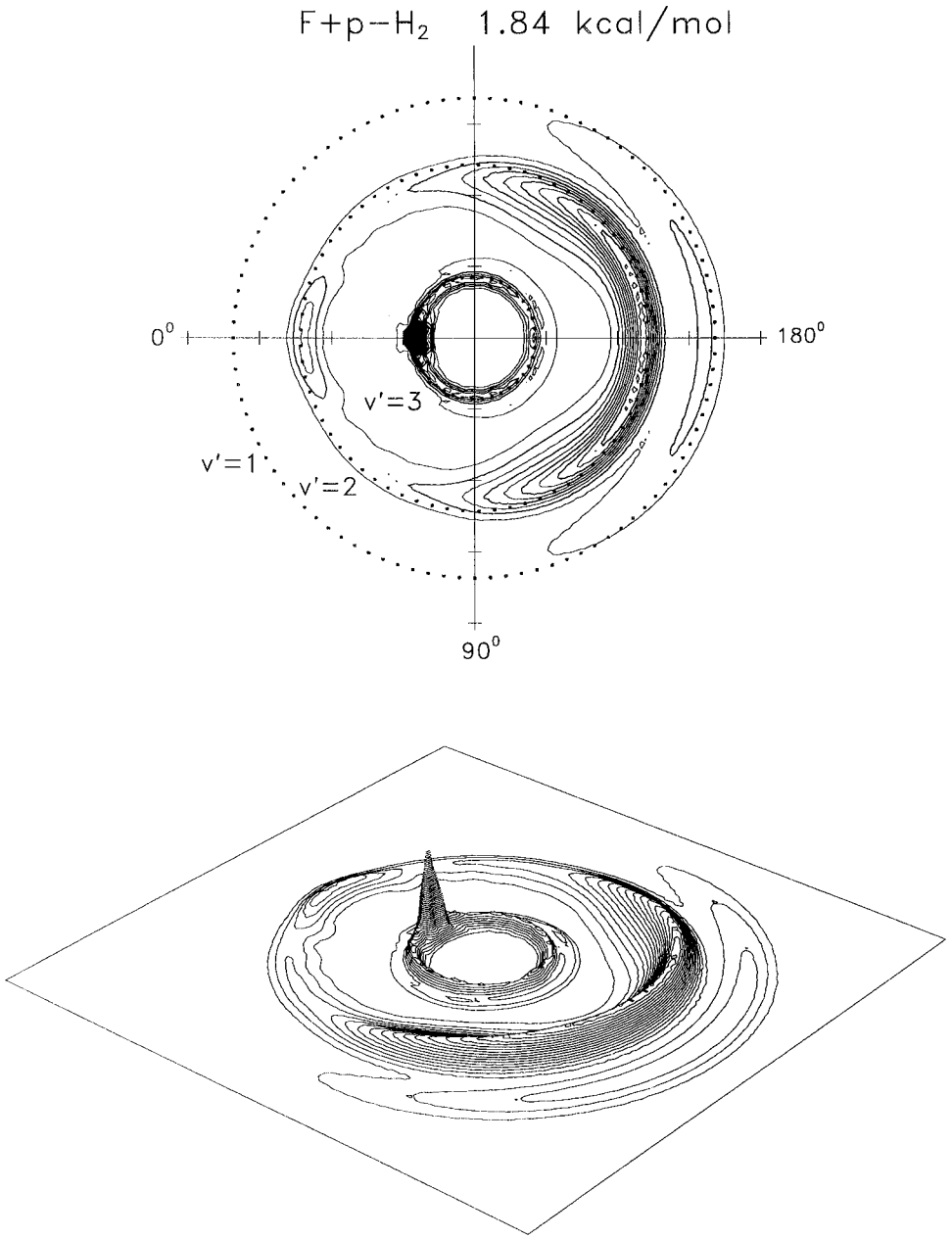

Figure 11. Theoretical scattering angle−recoil velocity contour polar map and 3D perspective for the F + *p*-H_2 reaction at 1.84 kcal mol^{-1} using the quantum mechanical v',j' resolved differential cross-sections of ref 43. The dotted circles represent the maximum HF recoil velocity at each vibrational state. The separation between the ticks of the axes is 200 m s^{-1}.

QM calculation would be of the order of the signal detected at *ca*. 55°. Since no upper bound of detectability at this range of LAB angles is given in the paper by Neumark *et al*.,[2] it is difficult to make a definitive statement on the compatibility of the theoretical simulations with the apparent absence of any $v' = 2$ forward scattering. However, it seems unlikely that a LAB $v' = 2$ forward scattering signal as high as the one obtained in the QM calculation on the SW PES would be lost in the experimental noise. Assuming a constant signal-to-noise ratio (*S*/*N*) at different LAB angles, the $v' = 2$ forward scattering would have been detectable in most of the experiments with *n*-H_2, although one might expect a poorer *S*/*N* ratio in the LAB angular region ∼−12° given the proximity of the F atom beam. It is not obvious the reason for the appearance of the $v' = 2$ forward scattering in the calculations, which, as stated before, seems to be present in other QM calculations. This might presumably be a consequence of the neglect of spin−orbit coupling in the *ab initio* calculation of the PES. The inclusion of this effect is expected to raise the barrier, and it is likely to cause a substantial decrease of the forward scattering into $v' = 2$ and, by analogy with the QCT results on the SW PES (see below), an increase of the $v' = 3$ sideways scattering.

The QCT v' resolved CM frame DCSs on the SW PES that were reported in ref 33 seemed to be in pretty good agreement with experiment. Although the forward peak was clearly smaller in magnitude and more confined into the forward scattering region, the general shapes of the DCSs were well accounted for, especially for $v' = 1$ and $v' = 2$. Figures 5 and 6 show the QCT simulations of the LAB ADs for the four experiments of Neumark *et al*. The corresponding QM distributions are also shown in these figures for comparison (dotted curves). It must be recalled that the QCT LAB ADs have been scaled using the same factors as were used for the QM simulations of each experiment, since both sets of theoretical results are directly comparable in absolute units.

As can be seen in Figures 5 and 6, the QCT simulations reproduce well the experimental ADs at the large LAB angles ($\Theta_{LAB} > 30°$). In fact, for all four experiments it is found that the QCT and QM calculations predict quite similar ADs for the HF products in $v' = 1$ and $v' = 2$ with $\Theta_{LAB} > 20°$. The

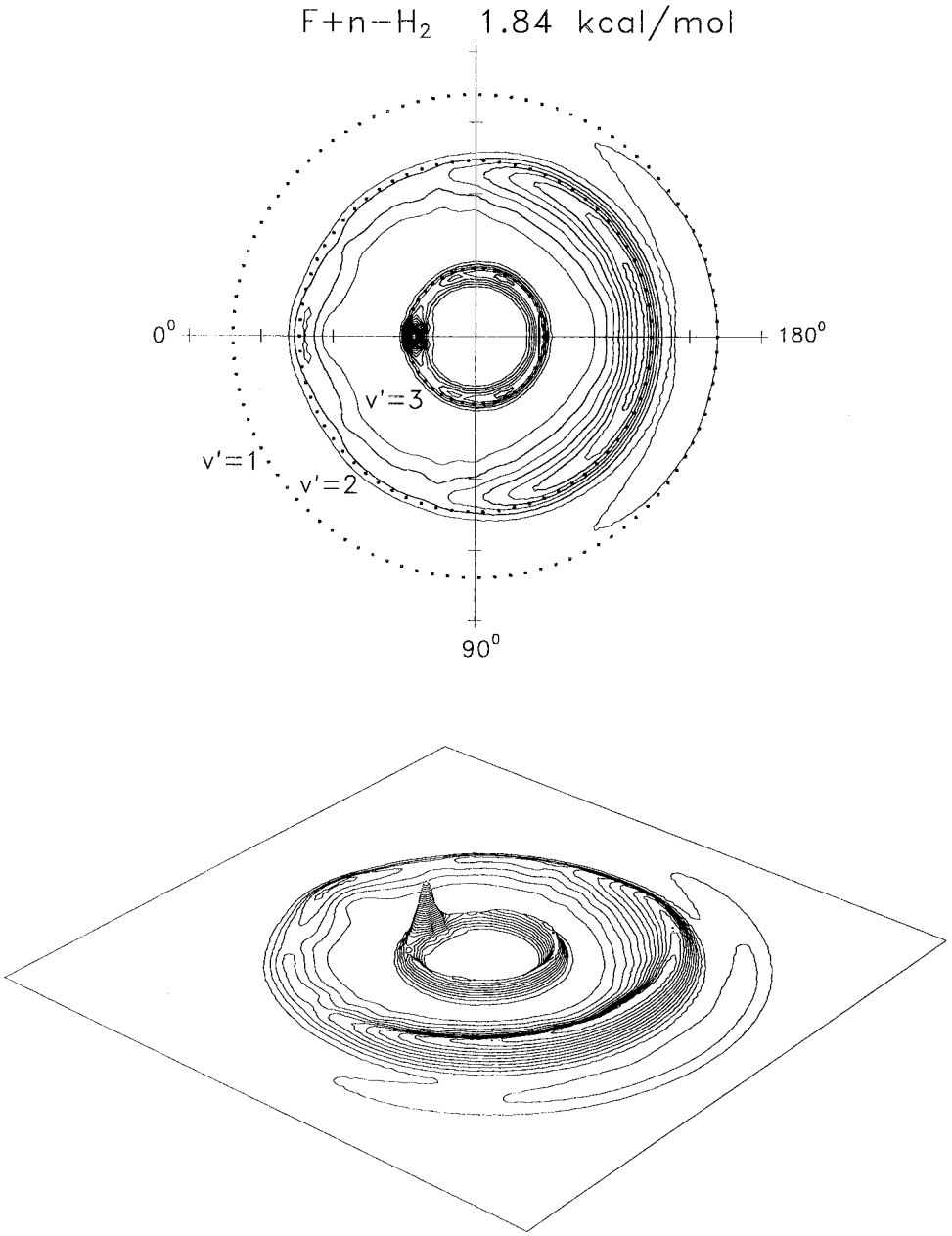

Figure 12. As in Figure 11, but for the F + *n*-H_2 reaction at 1.84 kcal mol^{-1}.

main differences between the QCT and QM simulations are found for the angular distribution of $v' = 3$ and for the forward scattering of $v' = 2$ which is enhanced in the QM calculation. The QCT calculation tends to overestimate the reactive yield at LAB angles close to the centroid, corresponding to $v' = 3$ CM sideways scattering, especially for the experiment at the two higher collision energies (Figure 6). On the other hand, the QCT simulations underestimate dramatically the forward scattering peak for $v' = 3$, the predicted intensity of which is roughly between 10% (in the experiment with F + *p*-H_2 at 1.84 kcal mol^{-1}) and 50% (for F + *n*-H_2 at 3.42 kcal mol^{-1}) of the experimentally observed value, in strong contrast to the QM calculation. Thus, the difference between the QCT and QM $v' = 3$ forward scattering is fully appreciated when the simulation of the raw experimental data is carried out.

This effect is closely related to a well-characterized limitation of the QCT approximation for this reaction, namely, the neglect of tunneling through the combined centrifugal and PES barriers, which has been discussed in previous work.[43] The analysis of the QM results clearly indicates that the forward scattering is almost exclusively due to the contribution of high angular momenta, whose values exceed considerably those classically allowed. A similar effect can also be envisaged for the $v' = 2$ forward scattering, and indeed the QCT calculations predict a much lower forward contribution from $v' = 2$ than the analogous QM calculations. By contrast, the QCT approximation gives an excess of $v' = 3$ sideways scattering which is underestimated in the QM calculations.

It is interesting to notice that, at first glance, a comparison of the QM, QCT, and experimental DCSs in ref 43 would lead to the impression that, overall, there is a somewhat better agreement between the QCT calculations and the experimental results in the CM frame. However, when the simulation of LAB ADs and TOF spectra (see below) is carried out, it becomes apparent that the QM calculations reproduce the experimental results far better than the QCT calculations. Once more, one should conclude that to obtain a definitive assessment of the quality of a theoretical scattering calculation on a given *ab initio* PES for this and other reactive systems, the most appropriate comparison with the experiment is in the LAB system.

B. Time-of-Flight Spectra. Figures 7−9 compare selected experimental and QM simulated time-of-flight spectra for the F + *p*-H_2 reaction at a collision energy of 1.84 kcal mol^{-1} (Figure 7) and for the F + *n*-H_2 reaction at 1.84 kcal mol^{-1}

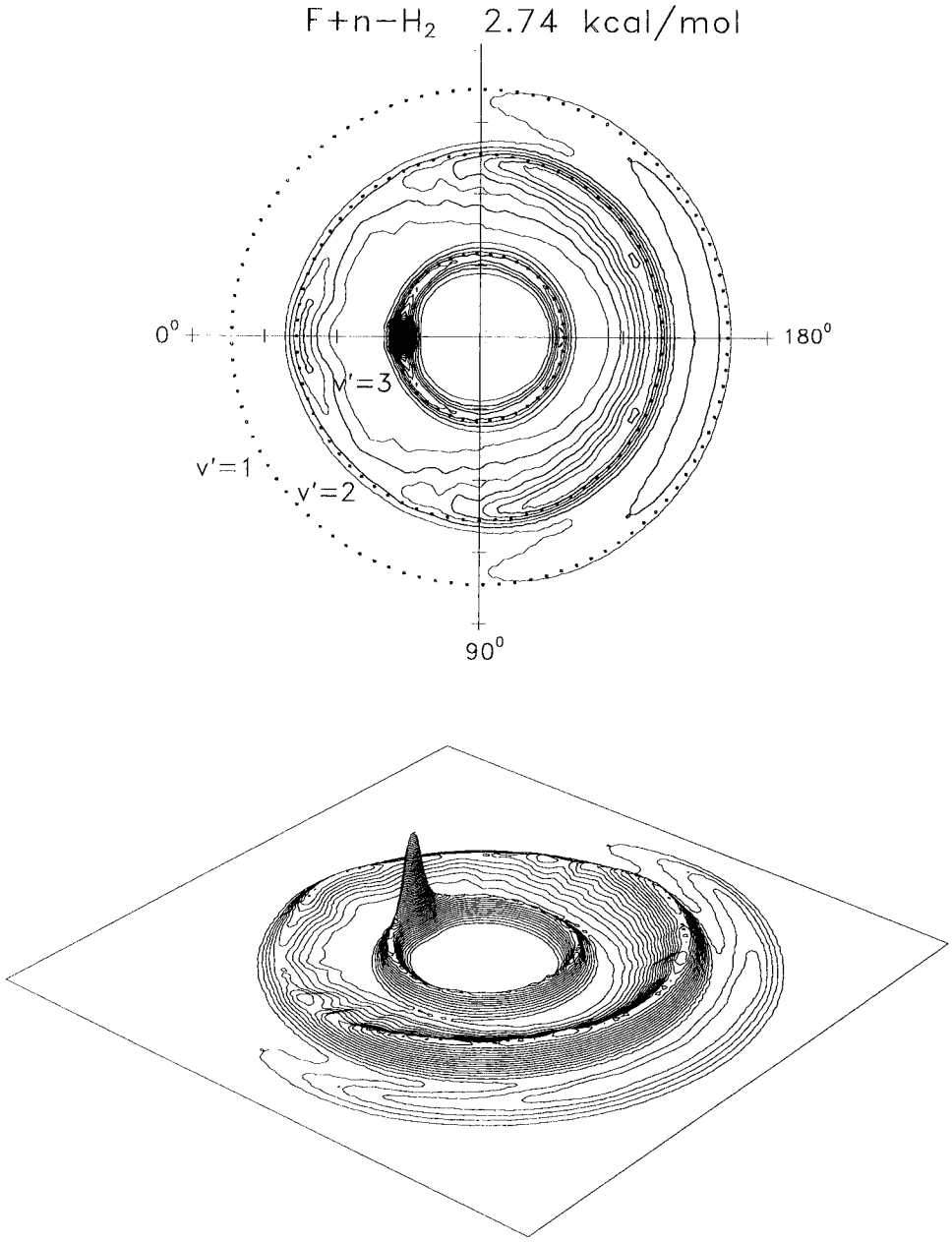

Figure 13. As in Figure 11, but for the F + *n*-H_2 reaction at 2.74 kcal mol^{-1}.

(Figure 8) and 3.42 kcal mol^{-1} (Figure 9). Overall, there is good agreement between the simulated and measured spectra throughout the LAB angular range. However, differences arise in the total intensity detected and in the relative heights of the different vibrational peaks in each TOF measurement.

In accordance with the results for the LAB ADs, the best agreement is obtained for the TOF spectra measured at large scattering angles ($\Theta_{LAB} \geq 30°$). The TOF spectra at intermediate LAB angles ($\Theta_{LAB} = 12-30°$) have one peak corresponding to scattering from $v' = 2$ and two peaks corresponding to the fast and slow LAB velocities of $v' = 3$. The $v' = 2$ peak is very well reproduced in all cases, but those of $v' = 3$ are clearly underestimated in the simulations, especially for the lowest collision energy. This confirms the inadequacy of the calculated QM $v' = 3$ sideways and backward scattering in the CM frame.

The TOF spectra at $\Theta_{LAB} = 8$ and 10° in each experiment have only one peak from $v' = 3$ and a small shoulder from HF(v'=2) scattered into CM angles between 30 and 55°. The simulated TOF spectra at $\Theta_{LAB} = 8°$ reproduce correctly the location, the shape and, to a large extent, the height of the measured $v' = 3$ peak. Only at 3.42 kcal mol^{-1} collision energy, the simulated peak seems to be slightly overestimated. In addition, the small $v' = 2$ shoulder is well-reproduced in the simulations, and this is in contrast with those carried out by Neumark *et al*. using their final set of CM parameters, which underestimate the contribution from this state at these LAB angles. As the Θ_{LAB} increases, the simulated LAB AD forward peak falls more rapidly than the experimental one (see Figures 3 and 4), and consequently, the QM simulation leads to a significant underestimation of the height of the TOF peak at $\Theta_{LAB} = 10°$.

The performance of the QCT calculations on the SW PES is illustrated in Figure 10, where the simulation of the TOF spectra from the F + *n*-H_2 at 3.42 kcal mol^{-1} are shown. It should be recalled that the QCT spectra have been scaled with the same factor as the corresponding LAB AD (see section II). The best agreement with the measurements is found again at large LAB angles. In the particular case of $\Theta_{LAB} = 38°$, the QCT simulation resembles the experiment even better than the QM simulation (Figure 9). The QCT simulation of the TOF measurement at 24° reproduces satifactorily the $v' = 2$ peak, but the $v' = 3$ peak is broader than the experimental one, indicating a significantly hotter $v' = 3$ rotational distribution in the QCT calculation. This effect is responsible for the

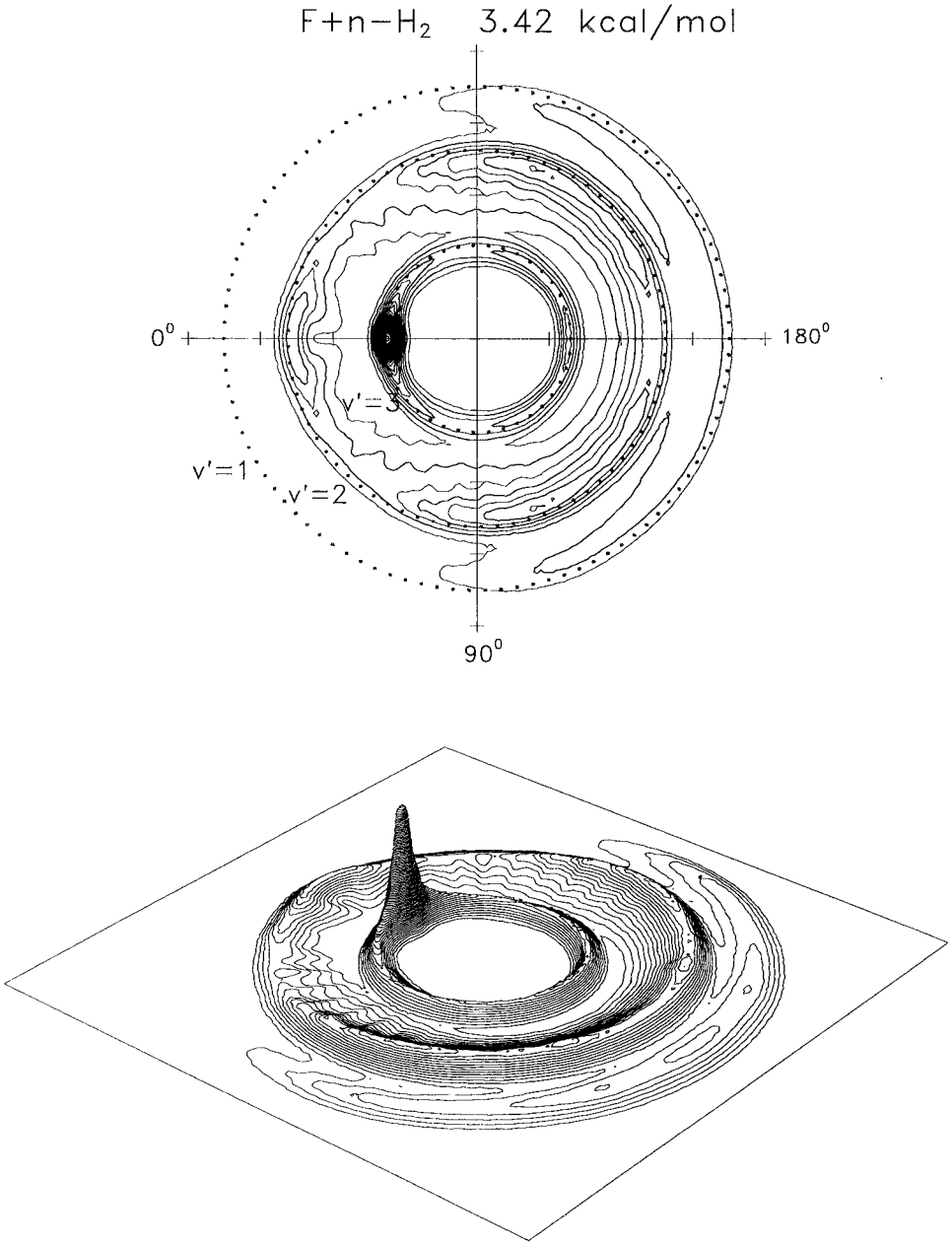

Figure 14. As in Figure 11, but for the F + *n*-H_2 reaction at 3.42 kcal mol^{-1}.

pronounced maximum in the LAB AD predicted by the QCT calculations at LAB angles around the centroid, $\Theta_{CM} \approx 25°$ (see Figure 6).

At LAB angles below 20°, the QCT calculated TOF spectra have a much smaller intensity than the experimental spectra, due to the inadequacy of the calculated QCT $v' = 3$ CM forward scattering. The shape of the peaks, however, is correctly reproduced in the QCT simulations, showing that the rotational distribution for the forward scattered HF(v'=3) is well accounted for in the QCT calculation.

C. Polar Maps. The summary of the information that could be experimentally obtained in the CM frame was presented as CM velocity flux contour maps as a function of the CM scattering angle in the original paper by Neumark *et al.*[2] For comparison, similar polar maps calculated from the QM fully v',j' resolved DCSs on the SW PES are depicted in Figures 11−14. As in their experimental counterparts, the most salient feature is the HF(v'=3) forward peak, which increases as collision energy increases and is higher for F + *p*-H_2 than for F + *n*-H_2 at the same energy. The main apparent discrepancy, already discussed in connection with the LAB ADs, is the presence of HF(v'=2) scattering in all directions in the CM frame, even with a shallow maximum in the forward region. In addition, the $v' = 3$ forward peaks are somewhat higher in the theoretical polar maps. A closer inspection of the experimental polar maps reveals that the $v' = 3$ scattering, at a given collision energy, increases as the CM angle decreases from 180°, whereas in the theoretical simulations, except for the forward peak, the scattering is nearly isotropic. This leads to a lack of $v' = 3$ CM sideways scattering, which is detected in the LAB system as the main discrepancy between theoretically simulated and experimental LAB ADs. The theoretical $v' = 1$ scattering seems to be more dispersed in CM angles than the experimental scattering, but given the low intensity of this state in the LAB frame the reliability of the experimentally extracted CM DCS is rather limited.

IV. Conclusions

More than 10 years after the cornerstone molecular beam experiment on the F + H_2 → HF + H reaction by the group of Y. T. Lee, a culmination of theoretical efforts in both quantum chemical calculations for the construction of *ab initio* potential energy surfaces and accurate quantum mechanical scattering

calculations has provided a scenario capable of reproducing the experimental observables at an unprecedented level of detail.

Although there are some interesting discrepancies between the theoretically simulated and experimental angular distributions and time-of-flight spectra of the HF products, the overall agreement is remarkably good. The limited performance of the classical calculations in reproducing the experimental measurements for this reaction has also been evidenced in the present work. Small adjustments of the potential energy surface, such as for example including spin−orbit effects, promise a final perfect agreement between theory and experiment. In particular, the inclusion of spin−orbit coupling is expected to cause an increase and broadening of the barrier that might prevent some of the higher total angular momenta contributing to the reaction. The consequence would be a slight decrease of the forward scattering in $v' = 3$ and $v' = 2$, and also perhaps an increase in the $v' = 3$ sideways scattering.

An important conclusion of this work is the importance of performing simulations of the experimental observables in the laboratory system to assess the quality of theoretical calculations.

For many years this milestone experiment was considered the one with the highest resolution for a chemical reaction. Subsequent improvements of experimental techniques during more recent years[39,41,42] and the use of new experimental approaches[44] have pushed forward the state-of-the-art, and practically fully resolved v',j' differential cross-sections can now be determined. The present and other works[44,50] show that *ab initio* simulations of high-resolution experiments are becoming feasible and should encourage new experimental efforts for an even more detailed understanding of the dynamics of chemical reactions.

Acknowledgment. We wish to gratefully dedicate this article to Professor Yuan T. Lee in his 60th anniversary. B.M.-H. acknowledges financial support through the program "Acciones para la incorporación de doctores y tecnólogos" from the Ministry of Education and Culture of Spain. J.F.C. acknowledges the E.C. for the award of a postdoctoral research position in Nottingham. The Spanish contribution to this work was financed by the DGICYT under Project No. PB95-0918-C02. The German part of this work received generous funding from the German Fonds der Chemischen Industrie. The Spanish−German exchange program "Acciones Integradas" is also acknowledged.

References and Notes

(1) Manolopoulos, D. E. *J. Chem. Soc., Faraday Trans.* **1997**, *93*, 673, and references cited therein.

(2) Neumark, D. M.; Wodtke, A. M.; Robinson, G. N.; Hayden, C. C.; Lee, Y. T. *J. Chem. Phys.* **1985**, *82*, 3045.

(3) Neumark, D. M.; Wodtke, A. M.; Robinson, G. N.; Hayden, C. C.; Shobatake, R.; Sparks, R. K.; Schafer, T. P.; Lee, Y. T. *J. Chem. Phys.* **1985**, *82*, 3067.

(4) For work up to 1980 see: Anderson, J. B. *Adv. Chem. Phys.* **1980**, *41*, 229, and references cited therein.

(5) Blais, N. C.; Truhlar, D. G. *J. Chem. Phys.* **1982**, *76*, 4490.

(6) Ron, S.; Baer, M.; Pollak, E. *J. Chem. Phys.* **1983**, *78*, 4414.

(7) Jellinek, J.; Baer, M.; Kouri, D. J. *Phys. Rev. Lett.* **1981**, *47*, 1588.

(8) Lee, K. T.; Bowman, J. M. *J. Phys. Chem.* **1982**, *86*, 2289.

(9) Baer, M.; Jellinek, J.; Kouri, D. J. *J. Chem. Phys.* **1983**, *78*, 2962.

(10) Abusalbi, N.; Shoemaker, C. L.; Kouri, D. J. *J. Chem. Phys.* **1984**, *80*, 3210.

(11) Hayes, E. F.; Walker, R. B. *J. Phys. Chem.* **1984**, *88*, 3318.

(12) Muckerman, J. T. In *Theoretical Chemistry. Advances and Perspectives*; Eyring, H., Henderson, D., Eds.; Academic Press: New York, 1981; Vol. 6A.

(13) Takayanagi, T.; Sato, S. *Chem. Phys. Lett.* **1988**, *144*, 191.

(14) Steckler, R.; Schwenke, D. W.; Brown, F. B.; Truhlar, D. G. *Chem. Phys. Lett.* **1985**, *121*, 475.

(15) Schwenke, D. W.; Steckler, R.; Brown, F. B.; Truhlar, D. G. *J. Chem. Phys.* **1986**, *84*, 5706.

(16) Lynch, G. C.; Steckler, R.; Schwenke, D. W.; Varandas, A. J. C.; Truhlar, D. G. *J. Chem. Phys.* **1991**, *94*, 7136.

(17) Mielke, S. L.; Lynch, G. C.; Truhlar, D. G.; Schwenke, D. W. *Chem. Phys. Lett.* **1993**, *213*, 11; **1994**, *217*, 173(E).

(18) Launay, J. M.; Le Dourneuf, M. *ICPEAC XVII*, Brisbane, July 1991; p 549.

(19) Launay, J. M. *Theor. Chim. Acta* **1991**, *79*, 183.

(20) Aoiz, F. J.; Herrero, V. J.; Nogueira, M. M.; Sáez Rábanos, V. *Chem. Phys. Lett.* **1993**, *204*, 359.

(21) Aoiz, F. J.; Herrero, V. J.; Nogueira, M. M.; Sáez Rábanos, V. *Chem. Phys. Lett.* **1993**, *211*, 72.

(22) Aoiz, F. J.; Bañares, L.; Herrero, V. J.; Sáez Rábanos, V. *Chem. Phys. Lett.* **1994**, *218*, 422.

(23) Aoiz, F. J.; Bañares, L.; Herrero, V. J.; Sáez Rábanos, V. *Chem. Phys.* **1994**, *187*, 227.

(24) Berry, M. J. *J. Chem. Phys.* **1973**, *59*, 6229, and references cited therein.

(25) Perry, D. S.; Polanyi, J. C. *Chem. Phys.* **1976**, *12*, 419. and references cited therein.

(26) Wurzberg, E.; Houston, P. L. *J. Chem. Phys.* **1980**, *72*, 4811.

(27) Heidner, R. F., III; Bott, J. F.; Gardner, C. E.; Melzer, J. E. *J. Chem. Phys.* **1980**, *72*, 4815.

(28) Atkinson, R.; Baulch, D. L.; Cox, R. A.; Hampson, R. F., Jr.; Kerr, S. A.; Troe, J. *J. Phys. Chem. Ref. Data* **1989**, *18*, 88.

(29) Weaver, A.; Metz, R. B.; Bradforth, S. E.; Neumark, D. M. *J. Chem. Phys.* **1990**, *83*, 5352.

(30) Weaver, A.; Neumark, D. M. *Faraday Discuss. Chem. Soc.* **1991**, *91*, 5.

(31) Zhang, J. Z. H.; Miller, W. H.; Weaver, A.; Neumark, D. *Chem. Phys. Lett.* **1991**, *182*, 283.

(32) Bradforth, S. E.; Arnold, D. W.; Neumark, D. M.; Manolopoulos, D. E. *J. Chem. Phys.* **1993**, *99*, 6345.

(33) Aoiz, F. J.; Bañares, L.; Herrero, V. J.; Sáez Rábanos, V.; Stark, K.; Werner, H.-J. *Chem. Phys. Lett.* **1994**, *223*, 215.

(34) Stark, K.; Werner, H.-J. *J. Chem. Phys.* **1996**, *104*, 6515.

(35) Manolopoulos, D. E.; Stark, K.; Werner, H.-J.; Arnold, D. W.; Bradforth, S. E.; Neumark, D. M. *Science* **1993**, *262*, 1852.

(36) Aoiz, F. J.; Bañares, L.; Herrero, V. J.; Sáez Rábanos, V.; Stark, K.; Werner, H.-J. *J. Phys. Chem.* **1994**, *98*, 10665.

(37) Aoiz, F. J.; Bañares, L.; Herrero, V. J.; Sáez Rábanos, V.; Stark, K.; Werner, H.-J. *J. Chem. Phys.* **1995**, *102*, 9248.

(38) Aoiz, F. J.; Bañares, L.; Faubel, M.; Martínez-Haya, B.; Rusin, L. Y.; Tappe, U.; Toennies, J. P. *Chem. Phys.* **1996**, *207*, 245.

(39) Faubel, M.; Rusin, L.; Schlemmer, S.; Sondermann F.; Tappe, U.; Toennies, J. P. *J. Chem. Phys.* **1994**, *101*, 2106.

(40) Faubel, M.; Martínez-Haya, B.; Rusin, L. Y.; Tappe, U.; Toennies, J. P. *Z. Phys. Chem.* **1995**, *188*, 197.

(41) Faubel, M.; Martínez-Haya, B.; Rusin, L. Y.; Tappe, U.; Toennies, J. P. *Chem. Phys. Lett.* **1995**, *232*, 197.

(42) Faubel, M.; Martínez-Haya, B.; Rusin, L. Y.; Tappe, U.; Toennies, J. P.; Aoiz, F. J.; Bañares, L. *Chem. Phys.* **1996**, *207*, 245.

(43) Castillo, J. F.; Manolopoulos, D. E.; Stark, S.; Werner, H.-J. *J. Chem. Phys.* **1996**, *104*, 6531.

(44) Schnieder, L.; Seekamp-Rahn, K.; Borkowski, J.; Wrede, E.; Welge, K. H.; Aoiz, F. J.; Bañares, L.; D'Mello, M. J.; Herrero, V. J.; Sáez Rábanos, V.; Wyatt, R. E. *Science* **1995**, *269*, 207.

(45) Schnieder, L.; Seekamp-Rahn, K.; Wreder, E.; Welge, K. H. *J. Chem. Phys.*, submitted for publication.

(46) Warnock, T. T.; Bernstein, R. B. *J. Chem. Phys.* **1968**, *49*, 1878; *J. Chem. Phys.* **1969**, *51*E, 4682.

(47) Neumark, D. M. Private communication.

(48) Pollard, J. E.; Trevor, D. J.; Lee, Y. T.; Shirley, D. A. *J. Chem. Phys.* **1982**, *77*, 4818.

(49) Neumark, D. M. Ph.D. Thesis; University of California, Berkeley, 1984.

(50) Alagia, M.; Balucani, N.; Cartechini, L.; Casavecchia, P.; van Kleef, E. H.; Volpi, G. G.; Aoiz, F. J.; Bañares, L.; Schwenke, D. W.; Allison, T. C.; Mielke, S. L.; Truhlar D. G. *Science* **1996**, *273*, 1519.